Size-Selected Zinc Sulfide Nanocrystallites: Synthesis, Structure, and Optical Studies

J. Nanda, Sameer Sapra, and D. D. Sarma*

Solid State and Structural Chemistry Unit, Indian Institute of Science, Bangalore 560 012, India

Nirmala Chandrasekharan and Gary Hodes

Department of Materials and Interfaces, The Weizmann Institute of Science, Rehovot 76100, Israel

Received September 13, 1999

We report the synthesis of three sizes of thioglycerol-capped precipitated ZnS nanocrystallites with relatively narrow size distributions, having average sizes of 1.8, 2.5, and 3.5 nm, respectively. These crystallites were extracted as free-standing powders which remain stable under normal atmospheric conditions and can be redispersed in suitable solvents. The nanocrystallite powders were characterized using X-ray diffraction (XRD), high-resolution transmission electron microscopy (HRTEM), electron diffraction (ED), energy dispersive analysis of X-rays (EDAX), and UV−vis optical absorption. The synthesized nanocrystallites show typical lattice spacings corresponding to the cubic phase of ZnS, as confirmed from HRTEM, ED, and XRD. The lattice-resolved structures within a single nanocrystallite show characteristic defects such as twinning and dislocations. We present a comparative analysis of the size of nanocrystallites obtained from X-ray diffraction and TEM. The position of the excitonic transitions as seen in the optical absorption spectrum of the nanocrystallites was compared with the predictions of various models that correlate the size versus band gap of these nanocrystallites.

I. Introduction

Synthesis of nanometer-sized semiconductor crystallites using various methods of colloid chemistry has been an area of intense activity over the past decade.[1] The emphasis has been mainly on the synthesis of semiconductor particles belonging to II−VI and III−V groups, which show significant quantum confinement effects.[2] Due to the strong confinement effects, the electrical and optical properties of these nanocrystallites vary significantly with their size. This ability to tune the physical properties of nanocrystallites makes them an important category of materials that can find potential applications in the area of optoelectronic devices.[3] Physical methods such as X-ray or electron beam lithography[4] that are commonly used for the fabrication of low-dimensional solids have inherent resolution limits that restrict these techniques from going down to the nanometer scale. On the other hand, the colloid chemistry route offers a simple means to synthesize such particles with good control of the size and more importantly the size distribution. There have been extensive reports in the past few years[5] demonstrating that, by changing the reaction conditions, that is, the concentration of the starting materials, the nature of the solvents, and the suitable capping/stabilizing agents, it is possible to synthesize a variety of nanocrystallites with different sizes. In most of these synthetic methods, one uses a capping agent which covalently binds to the surface atoms of the nanocrystallite and, thus, prevents them from forming a macroscopic bulk material. This stabilizes the nanocrystallites, making it possible to extract them as free-standing powders. The ability to extract such particles in a powder form which is stable under atmospheric conditions and the solubility of these nanocrystallite powders in suitable solvents for the purpose of making thin films without disrupting the integrity of the nanocrystals are two important factors for any real technological application of these nanocrystallites.

Bulk ZnS is an important inorganic material for light-emitting applications. ZnS doped with various transition

* Corresponding author. E-mail: sarma@sscu.iisc.ernet.in. Also at Jawaharlal Nehru Center for Advanced Scientific Research, Jakkur, Bangalore 560 064, India.

(1) (a) Alivisatos, A. P. *J. Phys. Chem.* **1996**, *100* (13) 226. (b) Weller, H. *Angew. Chem., Int. Ed. Engl.* **1993**, *32*, 41. (c) Henglien, A. *Chem. Rev.* **1989**, *89*, 1861.

(2) (a) Yoffe, A. D. *Adv. Phys.* **1993**, *42*, 173. (b) Kayanuma, Y. *Phys. Rev. B* **1988**, *38*, 9797.

(3) (a) Nanda, J.; Narayan, K. S.; Kuruvilla, B. A.; Murthy, G. L.; Sarma, D. D. *Appl. Phys. Lett.* **1998**, *72*, 1335. (b) Colvin, V. L.; Schlamp, M. C.; Alivisatos, A. P. *Nature (London)* **1994**, *370*, 354. (c) Dabbousi, B. O.; Bawendi, M. G.; Onitsuka, O.; Robner, M. F. *Appl. Phys. Lett.* **1995**, *66*, 1316.

(4) Kumar, A.; Biebuyck, H. A.; Whitesides, G. M. *Langmuir* **1994**, *10*, 1498.

(5) (a) Vossmeyer, T.; Katsikas, L.; Giersig, M.; Popovic, I. G.; Diesner, K.; Chemseddine, A.; Eychmuller, A.; Weller, H. *J. Phys. Chem.* **1994**, *98*, 7665. (b) Murray, C. B.; Norris, D. B.; Bawendi, M. G. *J. Am. Chem. Soc.* **1993**, *115*, 8706.

10.1021/cm990583f CCC: $19.00
Published on Web 03/09/2000

metal ions such as manganese is an efficient light-emitting material.[6] When such dopants are inserted in the nanometer-sized ZnS matrix, they exhibit interesting magnetooptical properties.[7] However, to get well-defined and optimized properties, it is necessary that the synthesized particles have a narrow size distribution, a higher crystallinity, and a lower defect density. The bulk of the studies on ZnS quantum crystallites in the past has been on those in the form of colloids, with the main interest being the study of their photocatalytic and photochemistry aspects.[8] The photocatalytic activity of these colloids is enhanced by varying the size of the crystallites, owing to the shift of the valence and conduction bands. Therefore, the redox potential of these crystallites changes as a function of their size. This has been demonstrated by Kanemoto et al.[9] in the case of photoreduction of carbon dioxide by ZnS nanocrystallites in organic solvents. Earlier, Rosseti et al.[10] and Henglein and co-workers[11] have studied the evolution of the optical and electronic properties of ZnS nanocrystallite colloids with size. These colloids, however, are stable only for a short duration of time, as they are prone to photocorrosion and also agglomerate into larger particles. There have also been attempts to obtain free-standing powders of ZnS nanocrystallites by using suitable surface-passivating agents such as thiols or surfactants[12] that covalently bind to the surface atoms of the nanocrystallites, making them stable under normal atmospheric conditions. However, most of these synthetic procedures, whether used to form colloids or capped free-standing powders, yield crystallites having a large size distribution. This is most commonly evident from the UV−vis optical absorption spectra, which, in many reported cases, are broad and featureless. In this article, we report the synthesis of three different sizes of ZnS nanocrystallites with an average size of 1.8, 2.5, and 3.5 nm and exhibiting sharp optical absorption edges and well-defined excitonic features. The particles were extracted as free-standing powders which readily dissolve in water and DMF; this allows one to make thin films of such nanoparticles on suitable substrates for potential device fabrications. The nanocrystallites were characterized by small-angle as well as wide-angle X-ray diffraction (XRD), transmission electron microscopy (TEM), electron diffraction (ED), energy dispersive analysis of X-rays (EDAX), and ultraviolet−visible (UV−vis) absorption. The high-resolution electron microscope (HREM) pictures of these crystallites show characteristic lattice-resolved planes corresponding to cubic ZnS. We also present a comparison of the sizes of the nanocrystallites obtained from TEM and X-ray diffraction. Analysis of the optical absorption spectra of the nanocrystallites was carried out with the help of different models that relate the optical band gap and the size of the crystallite.

(6) (a) Garlick, G. F. J.; Gibson, A. F. *J. Opt. Soc. Am.* **1949**, *39*, 935. (b) Ohring, M. *The material Science of Thin Films*; Academic: San Diego, CA, 1992.

(7) (a) Bhargava, R. N.; Gallagher, D.; Hong, X.; Nurmikko, A. *Phys. Rev. Lett.* **1994**, *72*, 416. (b) Kennedy, T. A.; Glaser, E. R.; Klien, P. B.; Bhargava, R. N. *Phys. Rev. B* **1995**, *52*, 14356.

(8) (a) Yanagida, S.; Masahisa, Y.; Shiragami, T.; Pac, C. *J. Phys. Chem.* **1990**, *94*, 3104. (b) Dunstan, D. E.; Hagfeldt, A.; Almegren, M.; Siegbahn, H. O. G.; Mukhtar, E. *J. Phys. Chem.* **1990**, *94*, 6797.

(9) Kanemoto, M.; Shiragami, T.; Pac, C.; Yanagida, S. *J. Phys. Chem.* **1992**, *96*, 3521.

(10) Rosseti, R.; Hull, R.; Gibson, J. M.; Brus, L. E. *J. Chem. Phys.* **1985**, *82*, 552.

(11) Henglein, A.; Gutierrez, M. *Ber. Bunsen-Ges. Phys. Chem.* **1983**, *87*, 852.

(12) (a) Nakaoka, Y.; Nosaka, Y. *Langmuir* **1997**, *13*, 708. (b) Kortan, A. R.; Hull, R.; Opila, R. L.; Bawendi, M. G.; Steigerwald, M. L.; Carroll, P. J.; Brus, L. E. *J. Am. Chem. Soc.* **1990**, *112*, 1327.

II. Experimental Section

A. Synthesis. We have used 1-thioglycerol as the capping agent to synthesize different sizes of ZnS nanocrystallites. Earlier, Nakaoka et al. used[12] a similar capping agent for synthesizing 1.5 nm ZnS nanoparticles. The synthetic route followed was a modification of the method adopted by Vossmeyer et al.[5] for preparing CdS nanocrystallites. We denote the synthesized particles as ZnS-1.8, ZnS-2.5, and ZnS-3.5 nm, corresponding to average diameters of 1.8, 2.5, and 3.5 nm, respectively.

1. Synthesis of ZnS-1.8. Zinc acetate dihydrate (2.2 mmol) and 5.2 mmol of 1-thioglycerol were dissolved in 50 mL of dimethyl formamide (DMF). Sodium sulfide nonahydrate (0.28 mmol) dissolved in 8 mL of water was added dropwise with stirring under an argon atmosphere. The solution was maintained at a pH of about 8 by adding 2 mL of 0.1 M NaOH solution. Subsequently, the solution was heated slowly and then refluxed for about 10−12 h. The refluxed solution was condensed using a rotary evaporator, and the particles were extracted by precipitation with the addition of acetone or alcohol to the concentrated solution. The crystallites were thoroughly washed several times with methanol followed by ether and then vacuum-dried. The extracted powders were found to dissolve readily in water.

2. Synthesis of ZnS-2.5. The synthetic procedure is similar to that of ZnS-1.8 except that the molar concentrations of 1-thioglycerol and sodium sulfide were changed to 3.5 and 0.55 mmol, respectively.

3. Synthesis of ZnS-3.5. About 2.2 mmol of zinc actetate and 1.56 mmol of thiourea were dissolved in 50 mL of DMF, and the solution was stirred under an argon atmosphere. 1-Thioglycerol (2.72 mmol) was added to this solution. The solution was refluxed for about 8−10 h. The particles were extracted as explained in Synthesis of ZnS-1.8.

B. X-ray Diffraction. The low-angle as well as wide-angle X-ray diffraction patterns were recorded using a Siemens D-5005 X-ray diffractometer. The nanocrystallite powders were pressed inside the sample holder, and the X-ray diffraction data were collected in the step scan mode. Since the diffracted intensities from such nanocrystallites are generally weak, all data were collected at a slow scan rate, with typically 20 s of data collection time for each step of 0.1°.

C. Transmission Electron Microscopy. Transmission electron microscopy (TEM) on the nanocrystallite samples was carried out using a JEOL-3010 electron microscope having an accelerating voltage of 300 kV with a point to point resolution of 1.7 Å. Samples for TEM were prepared by making a clear dispersion of the nanocrystallites in DMF and putting a drop of it on a carbon-coated copper grid. After a short time, the drop was removed from the grid using a soft tissue. The film was then dried under vacuum, leaving behind highly dispersed nanoparticles on the carbon grid.

D. Energy Dispersive Analysis of X-rays. The EDAX measurements on the synthesized nanocrystallite powders were performed using a JEOL-JSM 840A scanning electron microscope fitted with an EDAX unit. This gave a quantitative estimate of the composition of the nanocrystallites in atomic percentages.

E. UV−vis Optical Absorption. The optical absorption spectra of the nanocrystallites were measured using a Hitachi U-3000 UV−vis spectrophotometer. The nanocrystallite powders were dissolved in water and their optical absorption spectra were recorded. For bulk ZnS, we recorded the diffuse reflectance spectrum.

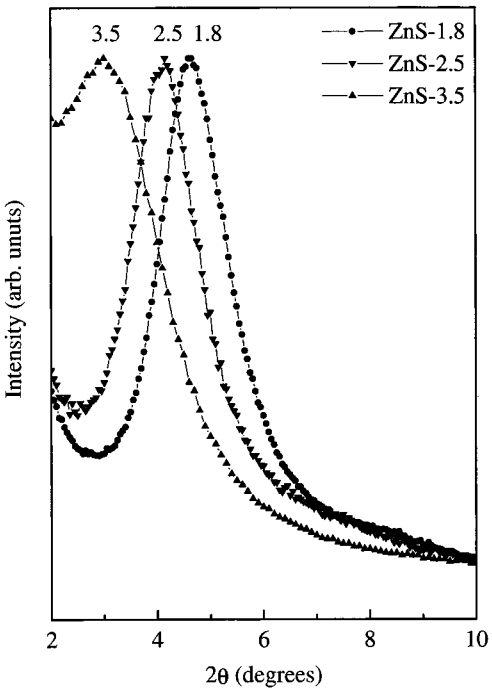

Figure 1. Small-angle X-ray diffraction of Zns-1.8, ZnS-2.5, and ZnS-3.5 nanocrystallites.

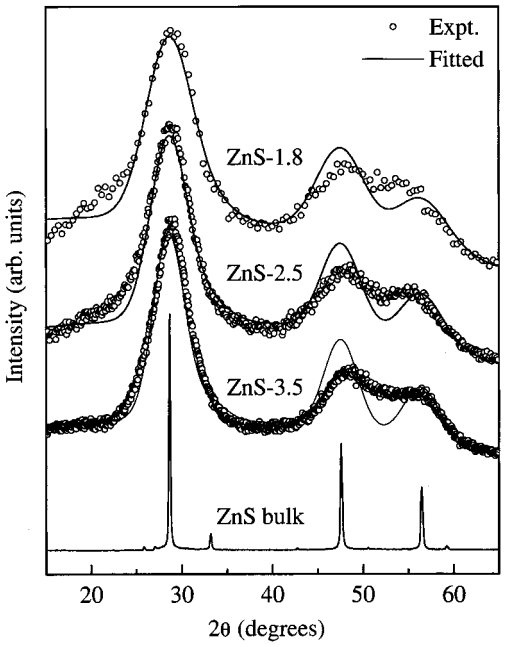

Figure 2. Wide-angle X-ray diffraction pattern of ZnS-1.8, ZnS-2.5, and ZnS-3.5 nanocrystallites. The filled circles show the experimental X-ray pattern, and the solid line, shows the fitting.

III. Results

A. X-ray Diffraction. Figure 1 shows the low-angle X-ray diffraction peaks corresponding to the three different sizes of the nanocrystallites. ZnS-1.8 has a characteristic peak at a 2θ value of 4.6°, and ZnS-2.5 and ZnS-3.5 have peaks at 4.1° and 2.9°, respectively. Such low-angle peaks have been earlier reported in the case of CdS nanocrystallites.[5] These nanocrystallite powders basically consist of tiny crystallites separated from each other by the ligand shell; while the individual nanoparticles are arranged randomly with respect to each other, the average distance between them is dominantly given by the diameter of the nanoparticle including the ligand shell. Thus, one expects a broad diffraction peak at the low-angle region arising from this characteristic separation between the nanoparticles, with the corresponding d value providing an estimate of the particle size. The average particle sizes, thus determined from the diffraction peaks in the low-angle region (Figure 1) are 1.8, 2.2, and 3.0 nm for ZnS-1.8, ZnS-2.5, and ZnS-3.5 nanocrystallites, respectively. The comparison of these values with the sizes determined from transmission electron microscopy will be discussed later in the text.

The wide-angle X-ray diffraction patterns of the nanocrystallites are shown in Figure 2. The XRD pattern of bulk ZnS corresponding to the cubic phase is also given for comparison. As expected, the XRD peaks of the nanocrystallites are considerably broadened compared to those of the bulk ZnS due to the finite size of these crystallites. However, all three sizes of the nanocrystallites have characteristic features matching the bulk cubic ZnS pattern. These diffraction features appearing at about 28.5°, 47.5°, and 56.3° correspond to the (111), (220), and (311) planes of the zinc blende phase of ZnS. To obtain more quantitative information, the bulk cubic XRD pattern was convoluted with Gaussian functions whose full widths at half maxima were determined from the Debye−Scherrer formula,[13] given by

$$L = \frac{0.9\lambda}{B \cos \theta}$$

where L is the coherence length, B is the full width at half maximum (fwhm) of the peak, λ is the wavelength of the X-ray radiation, and θ is the angle of diffraction. In the case of spherical crystallites, the relation between L and D, the diameter of the crystallite, is given by $L = {}^3/_4 D$. A fit to the experimental spectrum was obtained by using L as the fitting parameter. A suitable polynomial function was also included in the fitting program to take into account the X-ray background. As seen from Figure 2, for all three particle sizes, we obtained a reasonably good fit for the (111) peak, which lies at a 2θ value of 28.5° in the case of bulk cubic ZnS, by varying the parameter L. We notice that the fitted X-ray diffraction pattern does not match the experimental XRD pattern in the range of 20−25° because of the signal due to the amorphous glass substrate in the experimental XRD pattern. The optimum values of L obtained for ZnS-1.8, ZnS-2.5, and ZnS-3.5 nanocrystallites are 1.4, 1.7, and 2.0 nm, respectively. This translates to a crystallite size of 1.9, 2.3 and 2.7 nm, respectively. At higher 2θ values, there is a marked deviation between the fitted and the experimental X-ray diffraction patterns. The comparison of these sizes with the size determined from TEM and low-angle X-ray diffraction will be discussed later in the text.

B. Transmission Electron Microscopy. Figure 3a shows a low-magnification TEM image of ZnS-3.5 nanocrystallites. It shows an abundance of nearly spherical particles whose size distribution is given by the histogram shown in Figure 3b. It suggests that these

(13) Guinier, A. *X-ray Diffraction*; Freeman: San Francisco, CA, 1963.

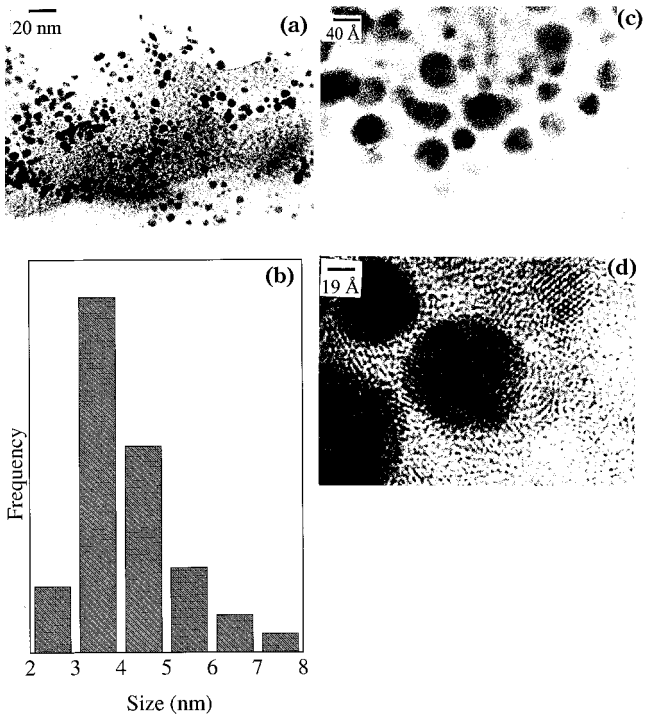

Figure 3. (a) Low-magnification TEM picture of ZnS-3.5 nanocrystallites. (b) Histogram showing the nanocrystallite size distribution. (c) High-resolution picture of ZnS-3.5 nanocrystallites showing lattice-resolved planes. (d) Magnified single ZnS-3.5 nanocrystallite showing twinning.

nanocrystallites have a mean particle size in the range of 3.5−4.0 nm. We have recorded higher magnification TEM pictures of individual crystallites, thus being able to resolve the lattice planes, as illustrated in Figure 3c. Careful observation of these lattice-resolved planes showed two sets of spacings, one having a *d* spacing of nearly 2.6 Å and the other having one of 3.0 Å. These spacings typically correspond to the (200) and (111) planes of the cubic ZnS phase, respectively. We have observed in the high-resolution pictures that a few of the crystallites exhibit twinning, having different sets of planes oriented in different directions inside a single crystallite. This is illustrated in Figure 3d. The low-magnification picture of ZnS-2.5 crystallites shows very fine particles with sizes ranging from 2 to 3 nm. In this case it was difficult to obtain a clear distribution of the particles, in contrast to the case of ZnS-3.5, due to finer particles and agglomeration of these particles when dried on the TEM grids. Nonetheless, one could observe nanocrystallites with the lattice planes resolved, as shown in Figure 4. The typical lattice spacing, as seen from the high-resolution picture is around 3.0 Å, corresponding to the (111) planes of the crystallite. Careful observation of these lattice planes in a single crystallite reveals the existence of structural defects, such as twinning and dislocations.[14] We show an example of a dislocation in ZnS-2.5 (Figure 4b), where one can clearly see a lattice plane terminating halfway in the crystallite (marked by an arrow) and the associated distortions of the neighboring lattice planes. It was not possible to obtain a reasonable TEM picture in the case of the smallest sized ZnS-1.8 crystallites because of the poor contrast. A selected area electron diffraction of ZnS-3.5 nanocrystallites is shown in Figure 5. As expected, in the case of nanocrystallites, the ED pattern shows a set of rings instead of spots due to the random orientation of the crystallites, corresponding to diffraction from different planes of the nanocrystallites. The ED pattern

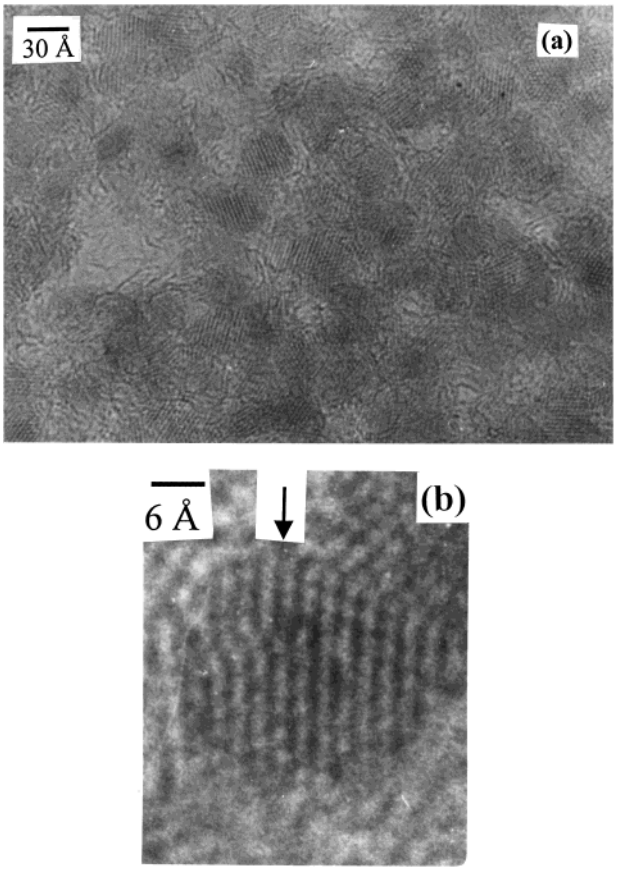

Figure 4. (a) High-resolution TEM picture of a ZnS-2.5 nanocrystallite showing lattice-resolved planes. (b) Magnified single ZnS-2.5 nanocrystallite showing dislocation.

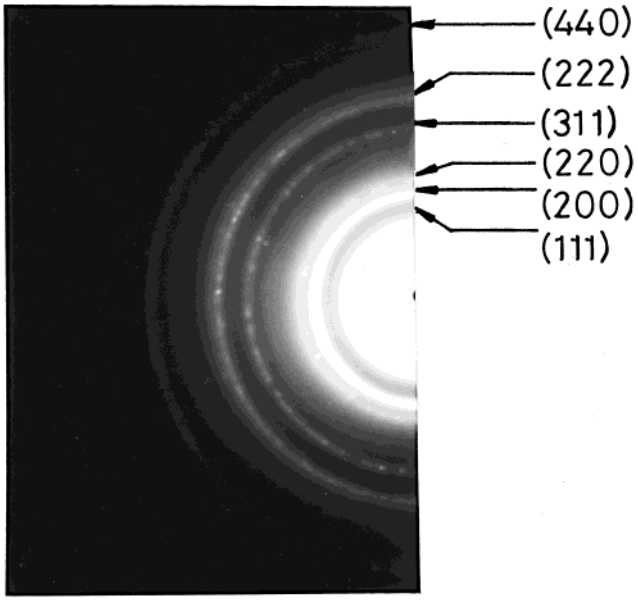

Figure 5. Selected area electron diffraction of ZnS-3.5 nanocrystallites. The rings correspond to specific lattice planes of the crystallite.

(14) West, A. R. *Solid State Chemistry and its Applications*: John Wiley & Sons: New York, 1984.

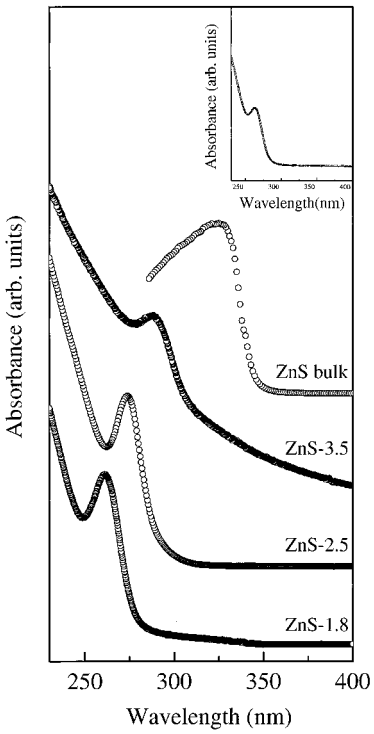

Figure 6. UV−vis optical absorption spectra of the ZnS nanocrystallites. The inset shows a typical absorption spectrum of the nanocrystalline film obtained by spin coating.

shows principally six rings which correspond to the (111), (200), (220), (311), (222), and (400) planes, respectively, of the cubic ZnS phase. To determine the lattice spacings of the nanocrystallites, the camera constant of the microscope was determined accurately by calibrating with a gold-coated grid. The lattice spacings are in agreement with the reported zinc blende structure of ZnS.

C. Energy Dispersive Analysis of X-rays. EDAX analysis of the powder samples of ZnS-1.8, ZnS-2.5, and ZnS-3.5 nanocrystallites shows zinc and sulfur to be in a stoichiometric atomic ratio within an accuracy of ±2%, this being the limit imposed by the uncertainties involved in the instrument calibration.

D. UV−vis optical absorption. The UV−vis optical absorption spectra of the three sizes of the nanocrystallites and of bulk ZnS (commercial sample) are shown in Figure 6. In the case of bulk ZnS, the optical absorption spectrum could not be recorded in the transmission mode. In this case, we recorded the diffused reflectance spectrum of the powdered ZnS. The absorption coefficient can then be calculated over the wavelength of interest by using the Kubelka−Munk function, which relates the absorption coefficient and the reflectance as[15]

$$K = \frac{2.303}{2d}\left(\frac{1 - R_\infty}{1 + R_\infty}\right) \log\left[\frac{R_\infty(1 - R_0 R_\infty)}{R_\infty - R_0}\right] \qquad (1)$$

where K is the absorption coefficient, R_∞ is the diffused reflectance, R_0 is the reflectance of the black background, and d is the thickness of the sample layer. The thus-obtained absorption spectrum of bulk ZnS shown in Figure 6 exhibits a sharp cutoff at 340 nm corresponding to 3.65 eV, which is the band gap[2] of bulk zinc blende ZnS. The absorption spectra of the nanocrystallite samples were recorded by dispersing the particles in the solvent and measured in the transmission mode. The nanocrystallites show sharp onset of absorption curves, exhibiting a systematic shift toward the higher energy, that is, lower wavelength (blue shift) with decreasing particle size. The absorption onset for each of the nanocrystallites is followed by a peak generally referred to as the excitonic peak. The excitonic peak positions of the ZnS-1.8, ZnS-2.5, and ZnS-3.5 are at 260, 272, and 288 nm, corresponding to 4.8, 4.55, and 4.3 eV, respectively. The long absorption tail in the case of ZnS-3.5 above 300 nm is due to scattering by the particles in the sol. It is interesting to note that solid thin films of the nanocrystallites made by spin coating the nanocrystallite powders dispersed in water/DMF on a quartz plate have similar sharp absorption features. A typical absorption spectrum of ZnS-1.8 crystallites on a quartz plate is shown in the inset of Figure 6. This opens up the possibility of constructing thin film devices from these nanoparticles with tunable electronic and optical properties.

(15) Kurtum, G. *Reflectance Spectroscopy: Principles, methods and application*; Springer-Verlag: Berlin-Heidelberg-New York, 1969.

Table 1. Comparison of the Nanocrystallite Sizes Obtained from X-ray Diffraction and Transmission Electron Microscopy (TEM)

type	small angle	wide-angle X-ray	TEM (nm)
ZnS-1.8	1.8	1.9	
ZnS-2.5	2.2	2.3	2.5
ZnS-3.5	3.0	2.7	3.5

IV. Discussion

Table 1 shows a comparison between the sizes of the nanocrystallites obtained from X-ray diffraction and TEM; it was not possible to estimate the size of the smallest nanocrystallite, ZnS-1.8, from TEM, as mentioned before. For all three samples, there is excellent agreement between the sizes obtained from small-angle and wide-angle X-ray diffraction data. The sizes obtained from X-ray diffraction measurements and TEM match reasonably well in the case of ZnS-2.5, while the size estimated from TEM in the case of ZnS-3.5 is somewhat larger than that estimated from X-ray diffraction results. Such differences between the sizes estimated from TEM and XRD have also been observed in the case of CdS nanocrystallites.[5] A possible explanation for this may be found in the observation that the larger nanoparticle, ZnS-3.5, exhibits a greater abundance of various defects in the crystallites, as illustrated by the transmission electron micrograph in Figure 3d. It is possible that the disagreement between the sizes obtained from XRD and TEM in the case of the larger nanocrystallite, ZnS-3.5, is due to this abundant presence of several crystalline domains oriented in different directions inside a single crystallite. The X-ray diffraction technique is sensitive to the dimensions of such individual local crystalline domains within a single nanocrystallite.

The simulated XRD pattern shown in Figure 2 fits reasonably well for the (111) reflections at about 28.5° for all three sizes of the crystallites. However, it deviates

substantially from the experimental spectrum at higher angles, with the experimental spectrum appearing to be much broader than the simulated spectrum. The simulation of the XRD pattern was carried out assuming a single size of the nanocrystallite instead of having a size distribution. Therefore, we explored the possibility of the disagreement at higher 2θ arising from this limitation by including a distribution of sizes for a given nanocrystallite within the simulation procedure. This, however, did not result in any significant improvement in the agreement between the simulated function and the experimental pattern. The reason for such disagreement between the experimental and fitted X-ray diffraction patterns is most probably the thermal broadening and various kinds of defects which are intrinsic in these types of nanocrystallites, grown by colloidal methods. It is well-known[13] that thermal effects contribute to the broadening of the X-ray diffraction peaks, with the magnitude of broadening increasing at higher values of 2θ. Moreover, defects such as stacking faults and distortions affect the diffraction line shape and position. The effect of stacking faults and distortions on the X-ray diffraction line shape of cubic and wurtzite ZnS was earlier studied in detail by Patterson[16] and Jagodzinski.[17] More recently, it has been shown by Bawendi et al. in the case of annealed CdSe nanocrystallites[18] that the inclusion of the thermal effect and stacking faults in the simulation of the X-ray diffraction pattern leads to a better agreement between the experimental and the simulated patterns.

The optical absorption feature of bulk ZnS shows a sharp absorption edge at 340 nm and has a broad feature in the far ultraviolet range which depends on the details of the band structure.[19] The absorption edges of the nanocrystallites are also sharp, indicating that the synthesized particles have relatively narrow size distributions. In the case of bulk ZnS, the excitonic binding energy[2] is about 34 meV; thus, the optical absorption spectrum of bulk ZnS at room temperature does not show the excitonic features, the excitonic binding energy being comparable to the thermal energy. On the other hand, as a consequence of the quantum confinement effect,[20] there is a significant increase in the binding energy of the excitons in the nanocrystallites. For example, in the case of CdS nanocrystallites, calculation of the exciton binding energy by Einevoll[21] by taking an infinite electron and hole barrier potential shows an increase of the exciton binding energy by few hundred millielectronvolts with a decrease in the size of the crystallite. This increased stability of the excitonic state in the nanocrystals allows the unambiguous observation of the excitonic spectral feature in the nanocrystallite optical absorption spectra even at room temperature, as clearly shown in Figure 6. These excitonic peaks correspond[2] to the first excitonic transition, the $1S_e-1S_h$ transition. The excitonic peak maximum shifts toward higher energy (lower wavelength) with a decrease in the nanocrystallite size due to the quantum size effect that systematically enhances the band gap with decreasing particle size. Though the binding energy of the exciton also increases with decreasing size due to an increasing Coulombic overlap enforced by enhanced spatial localization of the wave functions, the shift in the band gap with size dominates the spectral changes. Figure 7 shows the experimentally obtained dependence of the band-edge in these nanocrystallites as a function of the average particle size obtained from transmission electron micrographs. Since the size could not be estimated from TEM for the smallest size crystallites (ZnS-1.8), we use the size estimated from the X-ray diffraction pattern in this case. We have shown the error bar to the experimental points corresponding to the size distribution (about 10%) of the nanocrystallites. The error bar on the energy axis is the uncertainty in determining the band-edge position. The present experimental estimates agree with the values reported for similar sizes by Dunstan et al.[8b] and Nakaoka et al.[12] There are several theoretical models and calculations which correlate the band gaps of these nanocrystallites with their sizes. The most widely discussed ones in the recent literature are the effective mass approximation (EMA) first proposed by Efros[22] and later modified by Brus[23] and the semiempirical tight-binding (TB) calculations.[24]

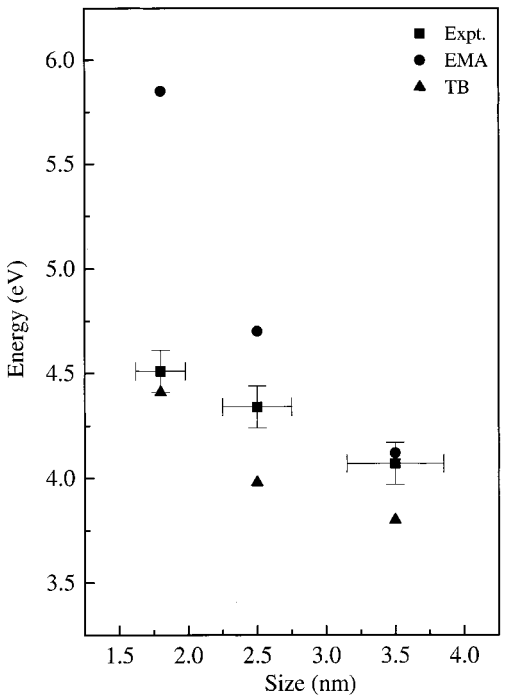

Figure 7. Experimental and calculated band gap versus size of ZnS nanocrystallites. The solid squares with error bars are the experimental points. The solid circles and triangles are the values calculated from the effective mass approximation (EMA) and tight-binding (TB) models, respectively.

We have shown the calculated excitation energies obtained from the EMA for the three different sizes of the crystallites in Figure 7 with filled circles.[25] It is apparent that the variation in the experimental result

(16) Paterson, M. S. *J. Appl. Phys.* **1952**, *23*, 805.
(17) Jagodzinski, H. *Acta Crystallogr.* **1949**, *2*, 298.
(18) Bawendi, M. G.; Kortan, A. R.; Steigerwald, M. L.; Brus, L. E. *J. Chem. Phys.* **1989**, *91*, 7282.
(19) The additional structure may be due to the transition between the bands lying at higher energies.
(20) Takagahara, T. *Phys. Rev. B* **1993**, *47*, 4569.
(21) Einevoll, G. T. *Phys. Rev. B* **1992**, *45*, 3410.
(22) Efros, AI. L.; Efros, A. L. *Sov. Phys. Semicond.* **1982**, *16*, 772.
(23) Brus, L. E. *J. Chem. Phys.* **1983**, *79*, 5566.
(24) Lippens, P. E.; Lannoo, L. *Phys. Rev. B* **1989**, *39*, 10935.

with the size of the nanocrystals is considerably weaker compared to the pronounced change in the calculated excitation energies within the EMA. It is well-known[2] that such a mismatch between the experiment and the calculation based on the EMA arises from the limitation of the theory and manifests itself more clearly for smaller sized nanocrystals. In this regard, tight-binding theories are expected to yield better results. However, the calculations based on such tight-binding approaches cannot be directly compared to the experimental excitonic band-edges, since the tight-binding approach does not take into account the Coulomb interaction between the electron and the hole. Thus, it is necessary to add the excitonic binding energies to the calculated band gaps obtained from the tight-binding analysis before any comparison is made. The excitonic binding energy for a given size of nanocrystallites can be easily estimated from the Coulomb term of the energy expression in the effective mass approximation. We have obtained the tight-binding estimates of the band gaps for ZnS nanocrystallites from ref 24 and incorporated the excitonic binding energies for the respective size of the nanocrystallites; these estimates are also shown in Figure 7 by solid triangles. We find that the dependence of the excitonic band-edge from the tight-binding approach is indeed less pronounced than that suggested by the EMA and is in better agreement with that of the experimentally observed ones. However, the values calculated from the TB model consistently underestimate the experimental energy positions for all sizes. At this juncture, it is worthwhile to discuss the limitation of both approaches in calculating the band gaps of such nanocrystallites. All three nanocrystallites synthesized in the present study have sizes less than the Bohr excitonic diameter of ZnS, which is around 5.5 nm.[2] The band dispersions deviate substantially from the parabolic nature, as assumed in the EMA at such a small crystallite size. Moreover, as the crystallite size is reduced, there is an increase in the electron and hole effective masses due to the decrease in the curvature of the top of the valence band and the bottom of the conduction band, while in the case of the EMA, the energies are calculated by taking the effective mass of the electron and the hole of the bulk solid. In the tight-binding calculations, the tight-binding parameters were obtained as a fitting to the bulk band structure at specific points of the Brillouin zone. Therefore, this model takes into account the band dispersion in a more realistic way, giving better agreement to the experimental points at small crystallite sizes. However, the band gap values calculated within the tight-binding approach are consistently smaller compared to the experimental values. This has been attributed[24] to the inability of the TB model to describe the lowest conduction band in a satisfactory way, particularly as a function of decreasing crystallite size.

In conclusion, we have reported the synthesis and characterization of three different sizes of ZnS nanocrystallites with relatively narrow size distributions. The average particle sizes of these crystallites were estimated using different techniques and found to be about 1.8, 2.5, and 3.5 nm. X-ray diffraction and high-resolution electron microscopy studies reveal that the synthesized particles have the zinc blende structure. The larger crystallites show intrinsic defects like twinning and dislocations which may explain the slight discrepancy between the sizes estimated from X-ray diffraction and TEM. The shift of the band gap with respect to the size of the nanocrystallites as observed in the optical absorption spectra of the nanocrystallites was compared with results from model calculations that relate the band gap to the size of the crystallites. The synthesis of such size-selected and well-characterized nanocrystallites of various sizes, obtained as stable free-standing powders, provides an opportunity not only for potential applications in areas such as photovoltaic devices but also for studying the size dependent optical and electrical properties of such nanocrystallites.

Acknowledgment. This project is funded by the Department of Science and Technology, Govt. of India, and the Ministry of Science, Israel, under the joint Indo−Israel scientific cooperation program. We thank Yitzak Matsai and Dr. K. S. Narayan for help with the TEM studies.

CM990583F

(25) The effective masses of the electron and hole, m_e^* and m_h^*, were taken to be 0.25 m_0 and 0.61 m_0 from Kane et al. *Phys. Rev. B* **1978**, *18*, 6849. m_0 is the free electron mass. The dielectric constant was taken to be 5.2.